Climate change causes functionally colder winters for snow cover-dependent organisms

Likai Zhu [1*], Anthony R. Ives [2], Chi Zhang[1], Yuanyuan Guo [1*] and Volker C. Radeloff[3]

Refugia are habitats that allow organisms to persist when the environment makes persistence impossible elsewhere. The subnivium—the interface between snowpack and ground—is an important seasonal refugium that protects diverse species from extreme winter temperatures, but its future duration is uncertain with climate change. Here, we predict that subnivium duration will decrease from 126 d (2010–2014) to 110 d (2071–2100), which we have inferred using past and future duration of frozen ground with snow cover (D_{sc}) derived from remotely sensed datasets and climate projections. Concomitantly, duration of frozen ground without snow cover (D_{fwos}) at mid-latitudes is predicted to increase from 35 d to 45 d, with notable increases in the western United States, Europe, the Tibetan Plateau and Mongolia. In most areas, increasing winter temperatures were more important than precipitation for decreasing D_{sc} and increasing D_{fwos}. Thus, counter-intuitively, warming climate will cause longer D_{fwos} at mid-latitudes, causing functional winter cooling for subnivium-dependent organisms.

Snow provides a thermally stable and humid space, the subnivium, due to its insulating capacity and low thermal conductivity[1,2]. Long-lasting snow cover promotes the overwintering survival of a wide range of species, which is reflected, for example, in the southern boundary of many northern plant species in temperate North America[3]: the southern boundary occurs where winter snow cover is intermittent and northern species cannot survive the freeze–thaw cycles that cause colder and more variable soil temperatures[4–6]. Climate change has altered the extent and duration of the subnivium and the freezing winter temperatures that the subnivium protects against[7–9]. Specifically, snow cover extent and duration has decreased in the Northern Hemisphere[10–13], and the duration of the frozen season per year has also decreased[14,15]. Although these general patterns in snow cover and frozen period have been documented, future subnivium duration at the global scale is still uncertain with climate change.

The duration of frozen ground with snow cover (D_{sc}) and without snow cover (D_{fwos}) can be strong predictors of the diversity of overwintering species such as plants[16,17], soil microbes[2], insects[18,19] and rodents[20–22]. However, D_{fwos} has been studied far less than D_{sc}, even though both are essential to defining the subnivium[6,16,23]. Predicting the consequences of global climate change on the subnivium is complicated, because warming climates result in two opposing trends. On the one hand, warming will decrease the duration of snow cover and thereby cause a deterioration of the subnivium. On the other hand, global warming is likely to decrease the length of winter and the duration of frozen ground. The ecological function of the subnivium depends at least in part on the difference between these two trends: how does the duration of frozen ground without snow cover change with a warming climate? This question is further complicated because snow cover depends not only on temperature but also on precipitation. Thus, predicting the future of the subnivium requires integrating multiple climatic factors.

We define D_{sc} as the number of days during the frozen season when frozen ground is covered by snow and D_{fwos} as the number of days when frozen ground is not covered by snow. D_{sc} indicates how

long organisms could be protected by the subnivium. D_{fwos} represents the length of the time period when organisms may be exposed to extremely low air temperatures during the winter because of the lack of the subnivium. We previously developed a dataset that captured the global average patterns of D_{sc} and D_{fwos} from 2000 to 2012[24] based on remotely sensed snow cover and freeze/thaw status datasets[25,26]. This 13 yr dataset, however, was too short to analyse trends through time, making it impossible to predict future changes. Given these limitations, our goals here are to (1) characterize changing patterns of the subnivium as measured by D_{sc} and D_{fwos} with a dataset from 1982 to 2014, (2) quantify effects of temperature and precipitation on changes to D_{sc} and D_{fwos}, and (3) use projections from 33 global climate models (GCMs) to predict changes in D_{sc} and D_{fwos} during the twenty-first century.

Results

D_{sc} and D_{fwos} are effective indicators of subnivium conditions. We derived D_{sc} and D_{fwos} annually at 5 km resolution from 1982 to 2014 across the globe by analysing freeze/thaw status, snow-cover status and the duration of the frozen season. Our accuracy assessment showed that remote sensing-derived D_{sc} and D_{fwos} values were consistent with those from station-based snow depth measurements (Pearson correlation coefficients of 0.90 and 0.91, respectively; Supplementary Fig. 1). Our analysis of the difference between ground temperatures and air temperatures (T_{diff}) showed that the average T_{diff} for the period of frozen ground with snow cover was larger than that for the period of frozen ground without snow cover (Fig. 1), indicating that frozen ground with snow cover provided effective insulation compared with bare frozen ground and that areas with higher D_{sc} and lower D_{fwos} probably exposed organisms in the subnivium to lower temperatures for a longer time.

In addition to snow cover duration, snow depth and density also influence subnivium conditions by changing the insulation capacity of the snowpack[2,27]. Snow depth and density are strongly and positively correlated (Supplementary Fig. 2), but they have opposite effects on the insulation capacity of a snowpack. Increased snow depth tends

[1]Shandong Provincial Key Laboratory of Water and Soil Conservation and Environmental Protection, College of Resources and Environment, Linyi University, Linyi, China. [2]Department of Integrative Biology, University of Wisconsin-Madison, Madison, WI, USA. [3]SILVIS Lab, Department of Forest and Wildlife Ecology, University of Wisconsin-Madison, Madison, WI, USA. *e-mail: zhulikai@lyu.edu.cn; yygpku@163.com
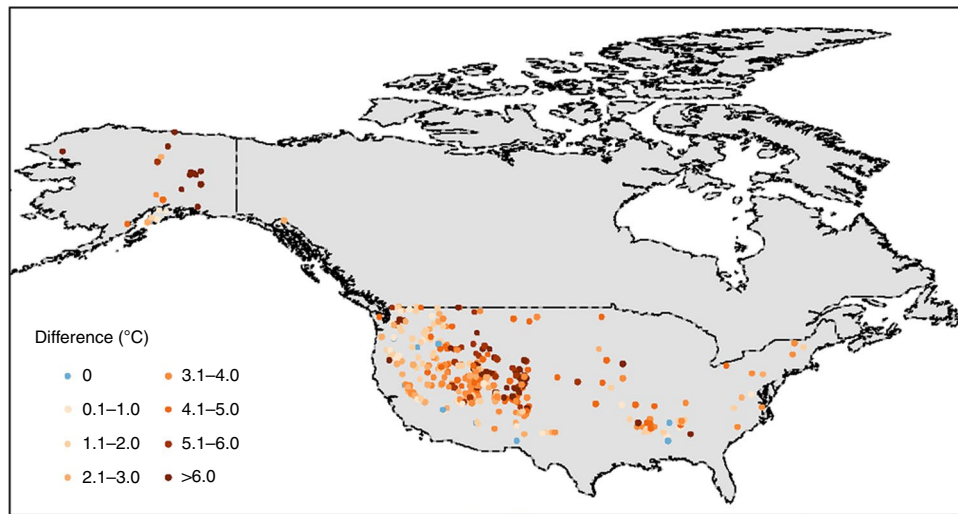
Fig. 1 | Average T_{diff} for the period of frozen ground with snow cover minus average T_{diff} for the period of frozen ground without snow cover. T_{diff} is calculated from weather station data by subtracting air temperatures from ground temperatures. The T_{diff} for periods with snow cover was generally larger than that for periods without snow cover.
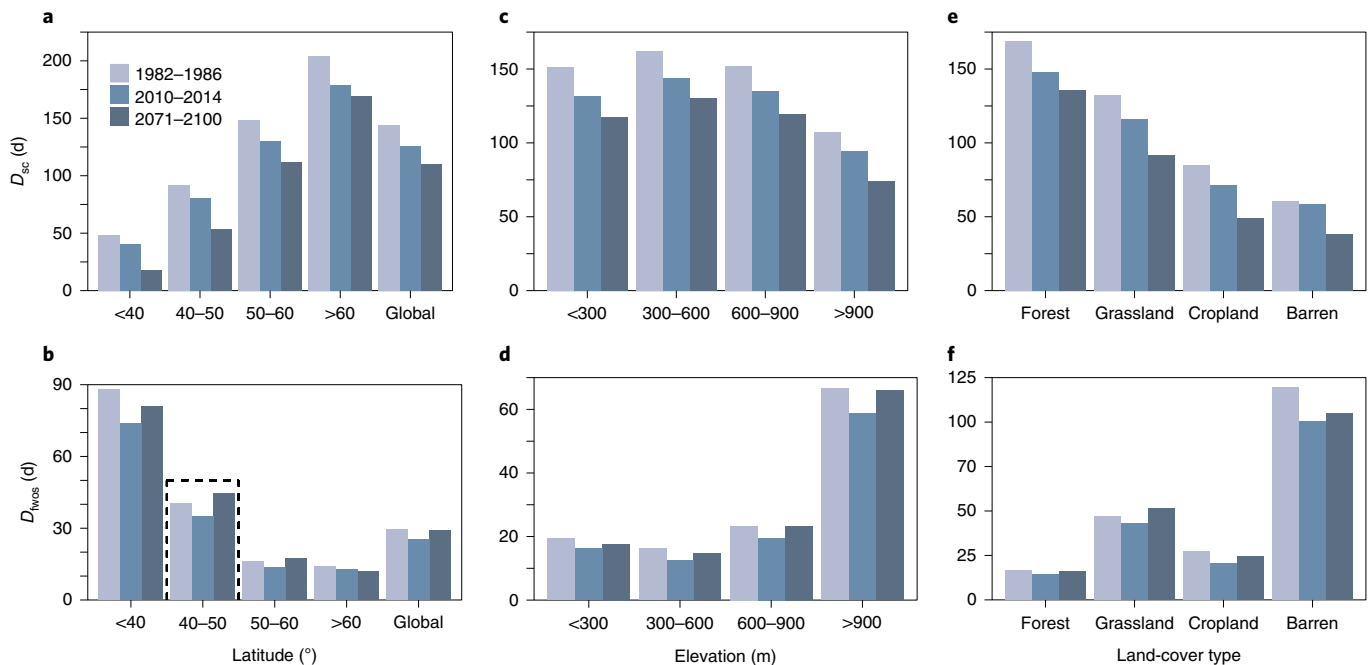

Fig. 2 | Observed and predicted values of D_{sc} and D_{fwos} for historical (1982–1986), current (2010–2014) and future (2071–2100) periods. a,b, D_{sc} (**a**) and D_{fwos} (**b**) averaged over latitude. D_{sc} experienced a consistent and widespread decrease and is predicted to decrease in the twenty-first century. D_{fwos} is predicted to increase at mid-latitudes as highlighted by the dashed line box. **c,d,** D_{sc} (**c**) and D_{fwos} (**d**) averaged over elevation. **e,f,** D_{sc} (**e**) and D_{fwos} (**f**) averaged over land-cover category.

to strengthen insulation capacity, while higher density increases thermal conductivity, which is inversely proportional to insulation capacity[28,29]. Modelling experiments show that the overall effect of increasing snow depth increases insulation capacity, even though it is typically accompanied by higher density[28]. This is also supported by the empirical evidence showing that ground temperatures are correlated positively with snow depth (Supplementary Fig. 3). Given the overall positive effect of snow depth on insulation capacity[28], we examined only the relationship between D_{sc} and mean snow depth during winter to test whether D_{sc} and D_{fwos} were good proxies of subnivium conditions. We found a strongly positive correlation between

D_{sc} and mean snow depth for almost all stations across the Northern Hemisphere (Supplementary Fig. 4). In summary, our measures of D_{sc} and D_{fwos} are effective indicators of the subnivium because they reflect subnivium temperatures and are closely correlated with snow depth, which influences subnivium conditions.

Changes in D_{sc} and D_{fwos} from 1982 to 2014. We compared the patterns of average D_{sc} and D_{fwos} for the past (1982–1986) and current (2010–2014) periods (Supplementary Fig. 5), and summarized them by latitude, elevation and land-cover type (Fig. 2). D_{sc} experienced a consistent and widespread decrease from 144 to 126 d, on
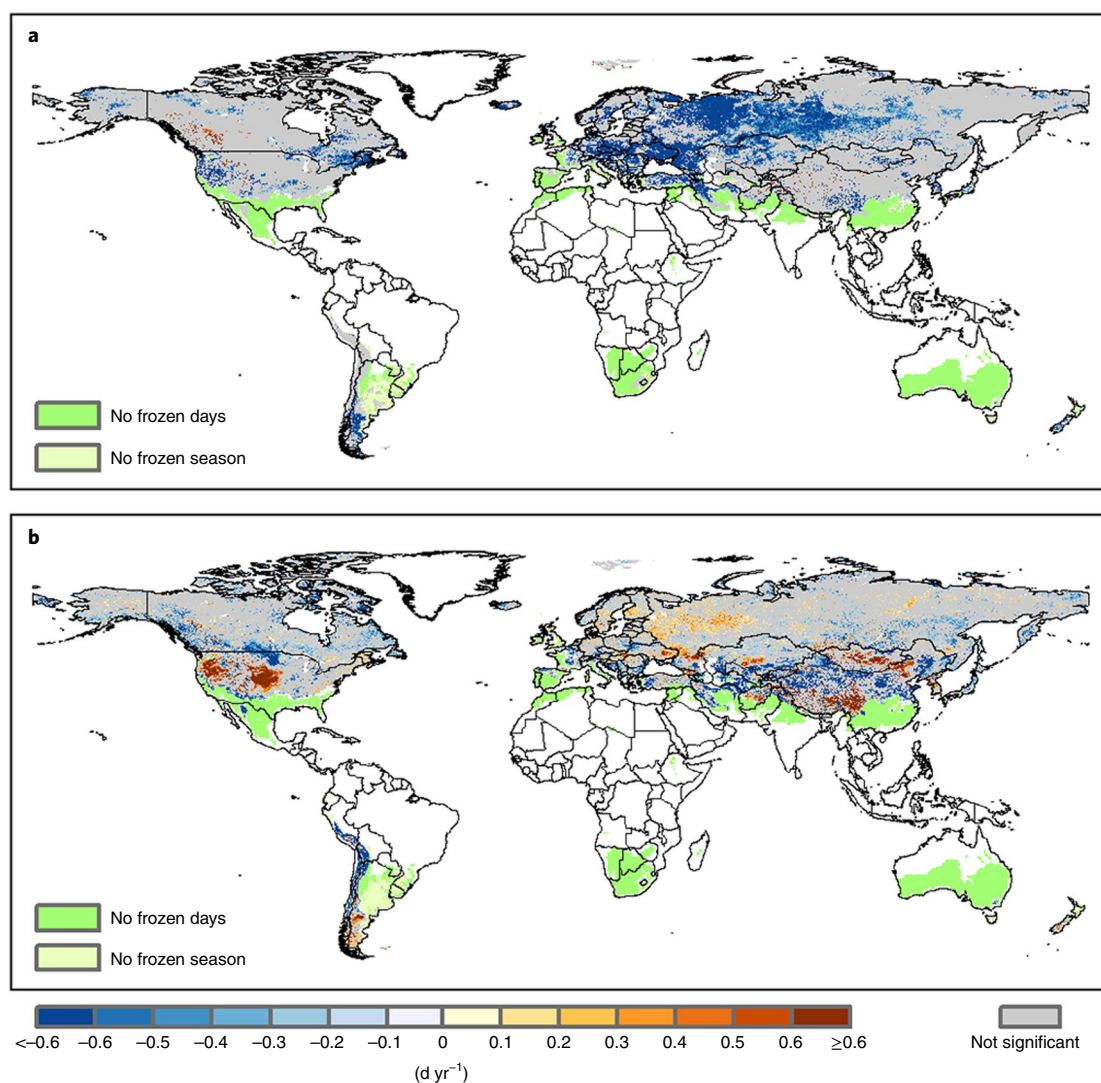
Fig. 3 | Global trends in D_{sc} and D_{fwos} from 1982 to 2014. a, Trends in D_{sc}. **b**, Trends in D_{fwos}. Pixels showing decreases in D_{sc} and increases in D_{fwos} are concentrated in the western United States, Europe, the southeastern Tibetan Plateau and Mongolia. Pixels with non-significant trends are displayed in grey.

average (Fig. 2a and Supplementary Figs. 5a and 6a). In contrast, D_{fwos} decreased most strongly at mid-latitudes, from 40 to 35 d, compared with changes at high latitudes where D_{fwos} declined only from 14 to 13 d (Fig. 2b and Supplementary Fig. 6a). However, there were notable regional exceptions to the overall decrease in D_{fwos}, especially in the western United States, Europe, the Tibetan Plateau and Mongolia (Supplementary Figs. 5b and 6b).

We fit time-series models to D_{sc} and D_{fwos} in each pixel to estimate trends from 1982 to 2014. We calculated the slope coefficient and showed only the pixels with trends that scored as significant at the 0.05 level according to Student's t-test. We found pixels with significant decreasing trends in D_{sc} mainly in the western United States, Europe, the southeastern Tibetan Plateau, Mongolia and southern Argentina (Fig. 3a), while pixels with significant increasing trends in D_{fwos} were observed in similar locations (Fig. 3b). Our trend analyses of mean snow depth for the frozen season also highlight significant decreases in the western United States and Europe (Supplementary Fig. 7).

Temperature and precipitation effects on D_{sc} and D_{fwos} from 1982 to 2014. To identify the effects of temperature and precipitation change on trends in D_{sc} and D_{fwos}, we analysed the Climate

Research Unit (CRU) datasets (1982 to 2015) at 0.5° resolution[30] and selected winter temperatures and precipitation as explanatory variables.

The widespread negative correlations between winter temperatures and D_{sc} indicated that warmer winters decreased D_{sc}, and the pixels with significant effects of winter temperature occurred at mid-latitudes in the conterminous United States, Europe, Mongolia and southern Argentina (Fig. 4a). The negative correlation was stronger especially at lower latitudes, because warming temperatures increased ablation, resulting in ephemeral snow conditions or shallow, patchy snow conditions and shorter snow persistence. Furthermore, we found positive correlations between winter precipitation and D_{sc} in mid-latitude areas such as in the central and western United States and in Mongolia, which indicates that increased snowfall is favourable for longer D_{sc} (Supplementary Fig. 8a).

The regressions of D_{fwos} against winter temperatures showed that winter temperatures were significantly and positively correlated with D_{fwos} for many pixels in the mid-latitudes, such as in the western United States, Europe and Mongolia, indicating that the number of days of bare frozen ground was, counter-intuitively, higher where temperatures were warmer (Fig. 4b). The correlation between
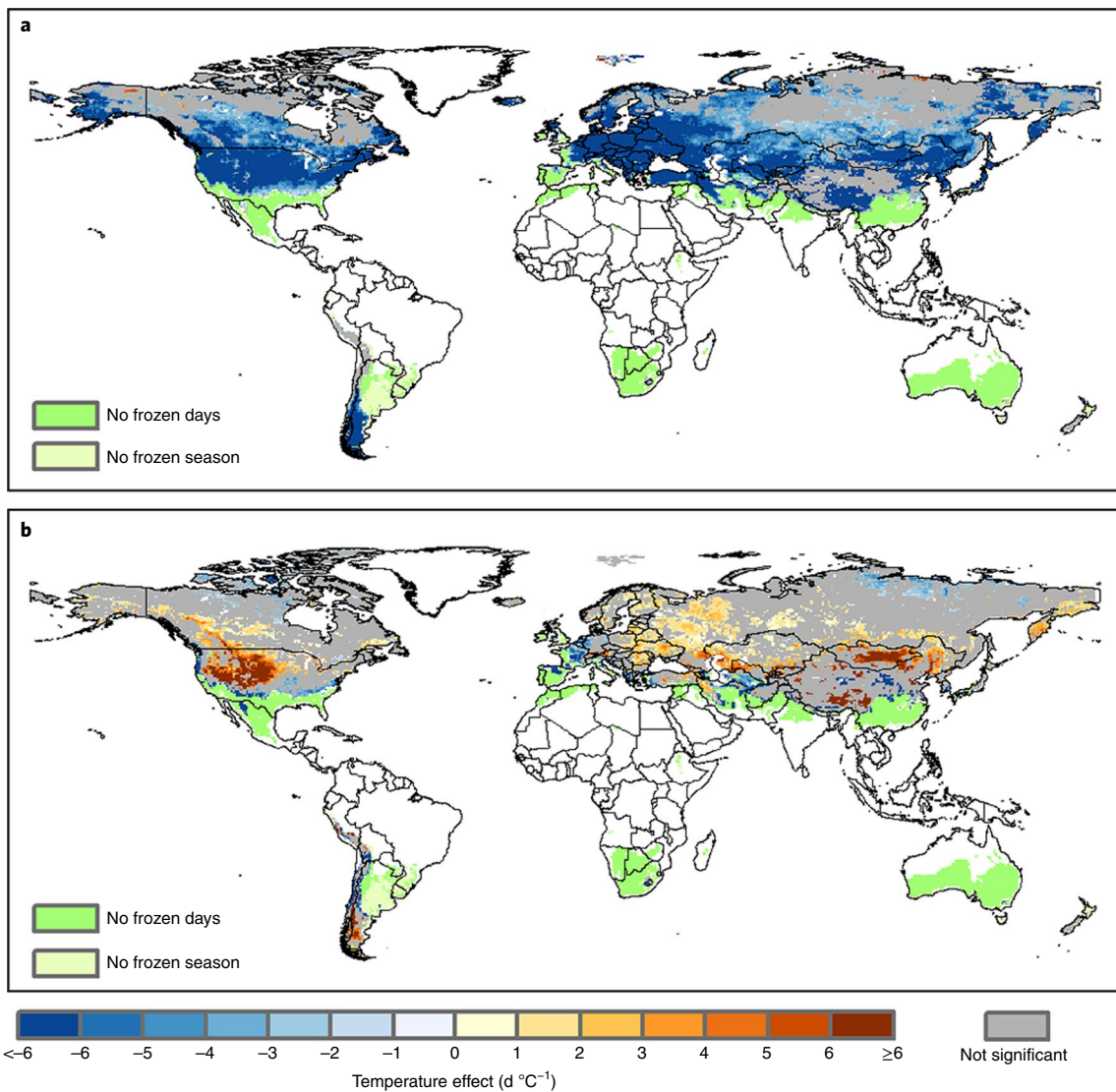
Fig. 4 | Global pattern of the effects of winter temperatures on D_{sc} and D_{fwos}. a, The regression coefficients of D_{sc} versus winter temperatures are generally negative, indicating that rising temperatures cause shorter D_{sc}. **b**, The regression coefficients of D_{fwos} versus winter temperatures were positive at mid-latitudes, indicating that rising temperatures caused longer D_{fwos}. Pixels with non-significant effects are displayed in grey.

D_{fwos} and winter precipitation was generally not significant, and negative correlation occurred only in Mongolia, indicating that increased snowfall there reduced D_{fwos} (Supplementary Fig. 8).

The relative importance of temperature and precipitation for D_{sc} and D_{fwos} varied across the globe (Fig. 5). Winter temperatures generally were more closely related to D_{sc} than precipitation was, especially in North America and Europe (Fig. 5a). However, in some regions, especially at high latitudes and in northwestern China, there was a stronger association between precipitation and D_{sc}. For D_{fwos}, the relationship with temperature was strong in Europe and western North America, but in the inland regions of Eurasia, the relationship with precipitation was stronger (Fig. 5b). Winter temperature influenced D_{sc} and D_{fwos} also via its interaction with winter precipitation. For example, increased precipitation offset the decrease in D_{sc} due to rising temperature in southern Canada and eastern Eurasia (Supplementary Fig. 9a). The regressions of D_{fwos} against the winter temperature–precipitation interaction variable indicated that increased precipitation could offset the increase in D_{fwos} due to increased temperatures in Mongolia and northern China (Supplementary Fig. 9b).

Both D_{sc} and D_{fwos} varied more with annual winter temperatures in relatively warmer climates (Supplementary Fig. 10). Specifically, the regression coefficients for the relationship between D_{sc} and winter temperature reached a minimum in regions where the mean annual winter temperature was relatively high. This implies that the subnivium in regions closer to the border of intermittent snow cover in winter is most sensitive to global warming, with small amounts of warming causing relatively large reductions in the duration of snow cover. D_{fwos} in these same regions was also more sensitive to climate warming, and even relatively minor winter warming caused large increases in the duration of conditions featuring frozen ground that is not covered by snow. Thus, for organisms that require the subnivium as a refuge from freezing conditions, global warming could increase the duration of their exposure to frozen days without refuge and hence make areas functionally colder.

Future predictions of D_{sc} and D_{fwos}. Our fitted regression models of D_{sc} and D_{fwos} against winter temperature and precipitation allowed us to predict changes in the subnivium from 2015 to 2100 using monthly Coupled Model Intercomparison Project phase 5 (CMIP5)
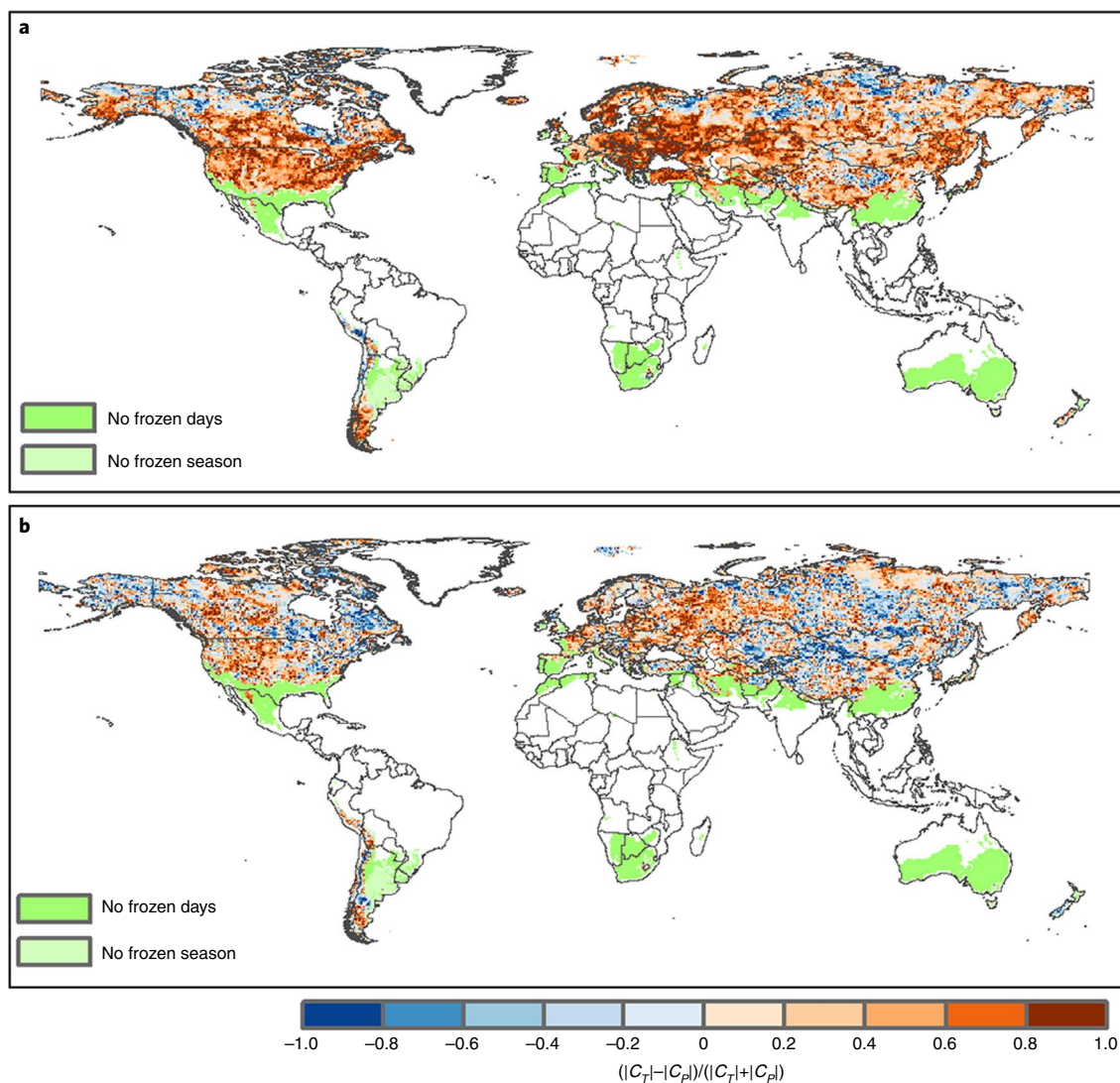
Fig. 5 | Global pattern of the relative importance of temperatures and precipitation for D_{sc} and D_{fwos}. This ratio varies from 1 when all of the variation is caused by temperature to −1 when all variation is caused by precipitation. **a**, The pattern for D_{sc} shows that winter temperatures generally were more closely related to D_{sc} changes than precipitation was. **b**, The pattern for D_{fwos} indicates that the relationships between D_{fwos} and temperature are stronger in Europe and western North America.

projections from 33 GCMs under the representative concentration pathway (RCP) 8.5 scenario[31]. Figure 6 shows differences in D_{sc} and D_{fwos} for the historical (1982–2014) and future (2071–2100) periods, and future changes are summarized by 1° latitude bins for each continent in Supplementary Fig. 11. D_{sc} is predicted to decrease from 136 to 110 d from the period 1982–2014 to 2071–2100 (Fig. 2 and Fig. 6a). The greatest decreases in D_{sc} are predicted to occur between 40° N and 50° N in North America and Asia (Supplementary Fig. 11a). D_{fwos} is predicted to increase in the western United States, the eastern Tibetan Plateau, Mongolia and Europe (Fig. 6b). The greatest predicted increases in D_{fwos} were between 40° N and 50° N for the Northern Hemisphere, from 39 to 45 d from 1982–2014 to 2071–2100 (Supplementary Fig. 11b).

Discussion
We inferred global changes in subnivium duration using past and future D_{sc} and D_{fwos} and revealed their relationships with winter temperature and precipitation. These changes will impact the many organisms that depend on the subnivium as a thermal refugium during winter.

Increases in D_{fwos} expose organisms to extremely low temperatures more frequently, thus threatening their survival. D_{fwos} has changed most rapidly at mid-latitudes, where higher temperatures have increased the number of days of frozen ground without snow cover. Interestingly, the regions in which D_{fwos} increased were also the regions in which D_{fwos} was related more strongly to temperature than to precipitation. Therefore, the increases in D_{fwos} are probably due to higher temperatures causing either midwinter or early spring snowmelt[12,32].

We documented the thermal benefit of snow cover, which indicated that decreased D_{sc} results in a functionally colder environment for organisms that depend on the subnivium. Similar to D_{fwos}, D_{sc} changed most at mid-latitudes and decreased especially in regions with relatively short winters. Also similar to D_{fwos}, rapid decreases in D_{sc} were more closely related to increasing winter temperature than to changes in precipitation, probably due to earlier thaws in spring and later freezes in fall[14] and also possibly due to midwinter snowmelt[11,12]. However, precipitation change could strengthen or offset temperature effects as indicated by our analysis of their interactions (Supplementary Fig. 9). Changes in precipitation are projected to
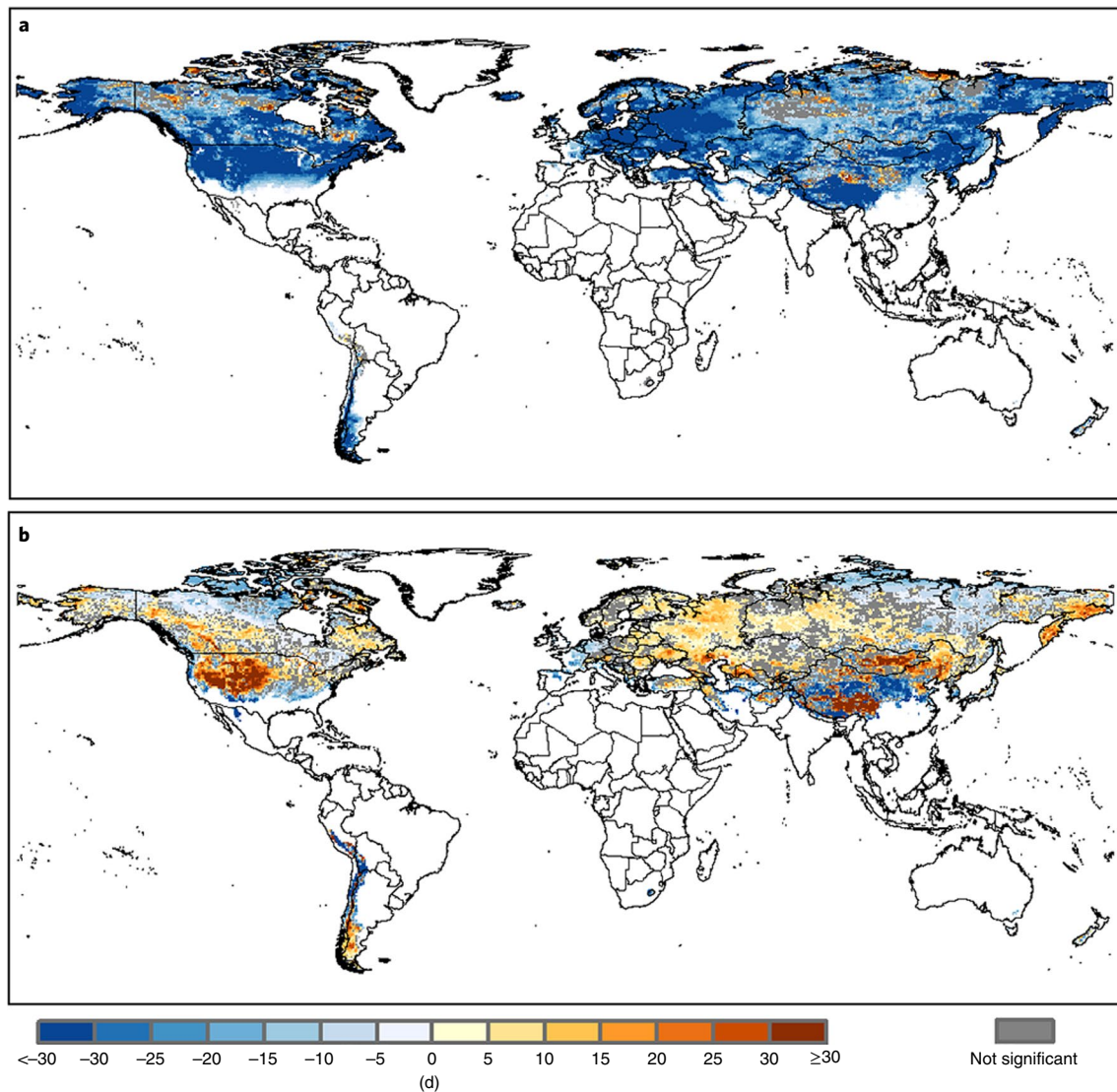
Fig. 6 | Global patterns of the differences in D_{sc} and D_{fwos} between the current (1982–2014) and future (2071–2100) periods. a, The pattern of the differences in D_{sc}, which shows widespread decreases in D_{sc}. **b**, The pattern of the differences in D_{fwos}, which suggests significant increases in D_{fwos} in mid-latitude areas. Pixels with non-significant differences in mean values at the 0.05 level according to Student's t-test are displayed in grey.

decrease in low to mid-latitudes but increase at high latitudes due to the contraction of the circumpolar vortex and a poleward shift of storm tracks[33]. These changes in winter precipitation will probably lead to reduced subnivium duration and longer duration of bare frozen ground.

A decrease of D_{sc} due to climate warming does not necessarily entail the deterioration of the subnivium, whose status is strongly influenced by various winter conditions, including the length of the winter season, ground status (frozen or thawed) and snow cover characteristics. Instead, increases in D_{fwos} may be more important, because they will make the environment functionally cooler for subnivium-dependent organisms by exposing them to extreme lower winter temperatures for a longer time. Interestingly, we found many areas at mid-latitudes with both decreasing trends for D_{sc} and increasing trends for D_{fwos}, including the western United States, Europe and Mongolia. Furthermore, we predict that D_{sc} and D_{fwos} will continue their current trends but at faster rates and over larger areas, extending, for example, into the Tibetan Plateau and northeastern China.

The projected decrease in D_{sc} and increase in D_{fwos} will probably be detrimental for many organisms that depend on the subnivium[2,7,8]. Species with limited dispersal abilities, including many insects, rodents, soil microbes and plants, will be especially vulnerable to the changes in the subnivium. Insects may perish when exposed to extremely cold temperatures and frequent freeze–thaw cycles[18,19]. Many rodents depend on the subnivium for thermal insulation, access to food resources and protection from avian predators such as owls and raptors[2,20]. The loss or deterioration of the subnivium is likely to affect population dynamics markedly by increasing predation risk due to longer exposure to predators and reducing access to available food resources due to ice formation[20,34]. Similarly, winter survival of microbes is negatively affected by lower soil temperatures caused by a lack of the subnivium, changing microbial composition and diversity, and nutrient mineralization rates[2,7]. Low temperatures also reduce the survival of vascular plants through frost damage to both aboveground tissue and root systems[5,6]. Furthermore, the loss of the subnivium will probably increase the number of freeze–thaw cycles, which decreases seed

viability of perennial plants[35]. However, future subnivium changes might have a positive effect on herbivores, because decreases in D_{sc} facilitate access to consumable plant materials. Ultimately, species will probably respond to changing winter conditions and the shrinking of the subnivium differently[36,37]. Many organisms with high dispersal ability may move towards the poles to areas where the subnivium is maintained[8,22]. Some species may also evolve to be more cold tolerant, although at least for plants, biogeographical patterns suggest that evolution of cold tolerance is very slow at the phylogenetic timescale[38].

Climate change causes a rapid decrease in D_{sc} and a concomitant increase in D_{fwos} especially in mid-latitude areas. The main reason for these trends has been warming in winter rather than changes in winter precipitation. The predicted future patterns for D_{sc} and D_{fwos} will continue recent trends, but at faster rates, with D_{sc} decreasing and D_{fwos} increasing, and trends are projected to occur much farther north in the Northern Hemisphere. Our research provides important information for biodiversity conservation in the light of climate change. Changes in both D_{sc} and D_{fwos} across the globe exhibit a strong spatial pattern, highlighting where threats to cold-adapted species are strongest and where active management to maintain the subnivium should be considered[39]. In particular, the lack of the subnivium at mid-latitudes will expose organisms more frequently to severe air temperatures and increased freeze–thaw cycles, and result in functionally colder winters for organisms that depend on the subnivium as a seasonal refugium.

Online content

Any methods, additional references, Nature Research reporting summaries, source data, statements of code and data availability and associated accession codes are available at https://doi.org/10.1038/s41558-019-0588-4.

References

1. Zhang, T. Influence of the seasonal snow cover on the ground thermal regime: an overview. *Rev. Geophys.* **43**, RG4002 (2005).
2. Pauli, J. N., Zuckerberg, B., Whiteman, J. P. & Porter, W. The subnivium: a deteriorating seasonal refugium. *Front. Ecol. Environ.* **11**, 260–267 (2013).
3. Curtis, J. T. *The Vegetation of Wisconsin: An Ordination of Plant Communities* (Univ. Wisconsin Press, 1959).
4. Brown, P. J. & DeGaetano, A. T. A paradox of cooling winter soil surface temperatures in a warming northeastern United States. *Agric. Meteorol.* **151**, 947–956 (2011).
5. Groffman, P. M. et al. Colder soils in a warmer world: a snow manipulation study in a northern hardwood forest ecosystem. *Biogeochemistry* **56**, 135–150 (2001).
6. Comerford, D. P. et al. Influence of experimental snow removal on root and canopy physiology of sugar maple trees in a northern hardwood forest. *Oecologia* **171**, 261–269 (2013).
7. Penczykowski, R. M., Connolly, B. M. & Barton, B. T. Winter is changing: trophic interactions under altered snow regimes. *Food Webs* **13**, 80–91 (2017).
8. Williams, C. M., Henry, H. A. L. & Sinclair, B. J. Cold truths: how winter drives responses of terrestrial organisms to climate change. *Biol. Rev.* **90**, 214–235 (2015).
9. Petty, S. K., Zuckerberg, B. & Pauli, J. N. Winter conditions and land cover structure the subnivium, a seasonal refuge beneath the snow. *PLoS ONE* **10**, e0127613 (2015).
10. Peng, S. et al. Change in snow phenology and its potential feedback to temperature in the Northern Hemisphere over the last three decades. *Environ. Res. Lett.* **8**, 014008 (2013).
11. Choi, G., Robinson, D. A. & Kang, S. Changing Northern Hemisphere snow seasons. *J. Clim.* **23**, 5305–5310 (2010).
12. Brown, R. D. & Robinson, D. A. Northern Hemisphere spring snow cover variability and change over 1922–2010 including an assessment of uncertainty. *Cryosphere* **5**, 219–229 (2011).
13. Hori, M. et al. A 38-year (1978–2015) Northern Hemisphere daily snow cover extent product derived using consistent objective criteria from satellite-borne optical sensors. *Remote Sens. Environ.* **191**, 402–418 (2017).
14. Kim, Y., Kimball, J. S., Zhang, K. & McDonald, K. C. Satellite detection of increasing Northern Hemisphere non-frozen seasons from 1979 to 2008: implications for regional vegetation growth. *Remote Sens. Environ.* **121**, 472–487 (2012).
15. Zhang, K., Kimball, J. S., Kim, Y. & Mcdonald, K. C. Changing freeze-thaw seasons in northern high latitudes and associated influences on evapotranspiration. *Hydrol. Process.* **25**, 4142–4151 (2011).
16. Blume-Werry, G., Kreyling, J., Laudon, H. & Milbau, A. Short-term climate change manipulation effects do not scale up to long-term legacies: effects of an absent snow cover on boreal forest plants. *J. Ecol.* **104**, 1638–1648 (2016).
17. Carlson, B. Z., Choler, P., Renaud, J., Dedieu, J. P. & Thuiller, W. Modelling snow cover duration improves predictions of functional and taxonomic diversity for alpine plant communities. *Ann. Bot.* **116**, 1023–1034 (2015).
18. Bale, J. S. & Hayward, S. A. L. Insect overwintering in a changing climate. *J. Exp. Biol.* **213**, 980–994 (2010).
19. Roland, J. & Matter, S. F. Pivotal effect of early-winter temperatures and snowfall on population growth of alpine *Parnassius smintheus* butterflies. *Ecol. Monogr.* **86**, 412–428 (2016).
20. Kausrud, K. L. et al. Linking climate change to lemming cycles. *Nature* **456**, 93–97 (2008).
21. Pedersen, S., Odden, M. & Pedersen, H. C. Climate change induced molting mismatch? Mountain hare abundance reduced by duration of snow cover and predator abundance. *Ecosphere* **8**, 1–8 (2017).
22. Sultaire, S. M. et al. Climate change surpasses land-use change in the contracting range boundary of a winter-adapted mammal. *Proc. R. Soc. B* **283**, 20153104 (2016).
23. Brown, R. D. & Mote, P. W. The response of Northern Hemisphere snow cover to a changing climate. *J. Clim.* **22**, 2124–2145 (2009).
24. Zhu, L., Radeloff, V. C. & Ives, A. R. Characterizing global patterns of frozen ground with and without snow cover using microwave and MODIS satellite data products. *Remote Sens. Environ.* **191**, 168–178 (2017).
25. Hall, D. K., Riggs, G. A., Salomonson, V. V., Digirolamo, N. E. & Bayr, K. J. MODIS snow-cover products. *Remote Sens. Environ.* **83**, 181–194 (2002).
26. Kim, Y., Kimball, J. S., McDonald, K. C. & Glassy, J. Developing a global data record of daily landscape freeze/thaw status using satellite passive microwave remote sensing. *IEEE Trans. Geosci. Remote Sens.* **49**, 949–960 (2011).
27. Thompson, K. L., Zuckerberg, B., Porter, W. P. & Pauli, J. N. The phenology of the subnivium. *Environ. Res. Lett.* **13**, 064037 (2018).
28. Ge, Y. & Gong, G. Land surface insulation response to snow depth variability. *J. Geophys. Res.* **115**, D08107 (2010).
29. Sturm, M., Holmgren, J., König, M. & Morris, K. The thermal conductivity of seasonal snow. *J. Glaciol.* **43**, 26–41 (2017).
30. Harris, I., Jones, P. D., Osborn, T. J. & Lister, D. H. Updated high-resolution grids of monthly climatic observations—the CRU TS3.10 Dataset. *Int. J. Climatol.* **34**, 623–642 (2014).
31. Maurer, E. P., Brekke, L., Pruitt, T. & Duffy, P. B. Fine-resolution climate projections enhance regional climate change impact studies. *Eos Trans. Am. Geophys. Union* **88**, 504–504 (2007).
32. Seager, R. & Vecchi, G. A. Greenhouse warming and the 21st century hydroclimate of southwestern North America. *Proc. Natl Acad. Sci. USA* **107**, 21277–21282 (2010).
33. McCabe, G. J. & Wolock, D. M. Long-term variability in Northern Hemisphere snow cover and associations with warmer winters. *Climatic Change* **99**, 141–153 (2010).
34. Korslund, L. & Steen, H. Small rodent winter survival: snow conditions limit access to food resources. *J. Anim. Ecol.* **75**, 156–166 (2006).
35. Connolly, B. M. & Orrock, J. L. Climatic variation and seed persistence: freeze–thaw cycles lower survival via the joint action of abiotic stress and fungal pathogens. *Oecologia* **179**, 609–616 (2015).
36. Kreyling, J. Winter climate change: a critical factor for temperate vegetation performance. *Ecology* **91**, 1939–1948 (2010).
37. Fountain, A. G. et al. The disappearing cryosphere: impacts and ecosystem responses to rapid cryosphere loss. *Bioscience* **62**, 405–415 (2012).
38. Hawkins, B. A., Rueda, M., Rangel, T. F. & Field, R. Community phylogenetics at the biogeographical scale: cold tolerance, niche conservatism and the structure of North American forests. *J. Biogeogr.* **41**, 23–38 (2014).
39. Zuckerberg, B. & Pauli, J. N. Conserving and managing the subnivium. *Conserv. Biol.* **32**, 774–781 (2018).

Acknowledgements

Author contributions

L.Z., A.R.I. and V.C.R. designed the study. L.Z., A.R.I., C.Z., Y.G. and V.C.R. analysed data. L.Z., A.R.I., C.Z., Y.G. and V.C.R. wrote the paper.

Competing interests

The authors declare no competing interests.

Additional information

Supplementary information is available for this paper at https://doi.org/10.1038/s41558-019-0588-4.

Correspondence and requests for materials should be addressed to L.Z. or Y.G.

Reprints and permissions information is available at www.nature.com/reprints.

Publisher's note Springer Nature remains neutral with regard to jurisdictional claims in published maps and institutional affiliations.

Methods

Deriving global D_{sc} and D_{fwos}. We determined land surface freeze/thaw status and the duration of the frozen season using the extended NASA MEaSUREs Global Record of Daily Landscape Freeze/Thaw Status dataset (FT-ESDR) (1982–2016) from the SMMR, SSM/I and SSMIS sensors[40]. This dataset is available at a 25 km spatial resolution from 1982 to 2015, and it has been generated by a refined algorithm with larger spatial extent compared with the previous versions. The dataset has high classification accuracies of 90.3% and 84.3% for evening and morning overpass retrievals, respectively. The long-term records have been widely used to identify freeze–thaw cycling, indicate climate change and define frozen temperature constraints to ecological processes[14,15,41]. We wrote Python code to automatically download the FT-ESDR dataset from the Numerical Terradynamic Simulation Group website (http://luna.ntsg.umt.edu/data/FT_ESDR/).

We used the JAXA Satellite Monitoring for Environmental Studies (JASMES) snow dataset at a 5 km spatial resolution from 1982 to 2016 to determine snow-cover status. This dataset is produced from Advanced Very High Resolution Radiometer (AVHRR) and Moderate Resolution Imaging Spectroradiometer (MODIS) radiances for five spectral bands using a decision tree algorithm with multiple thresholds[13]. Compared with other snow cover products (for example, the MODIS snow cover product and the NOAA Interactive Multisensor Snow and Ice Mapping System (IMS) snow cover product)[42], the JASMES dataset has both higher spatial resolution and a longer time span. Additionally, the dataset has a more temporally stable and higher producer's accuracy, which makes it advantageous for trend analyses.

To derive D_{sc} and D_{fwos}, first we determined the start and end of the frozen season annually on a pixel basis (Supplementary Fig. 12). For the Northern Hemisphere, the start of the frozen season was defined as the middle day of the first period of 15 consecutive days from September to February for which at least 8 days were classified as frozen. The end of the frozen season was defined as the middle day of the first period of 15 consecutive days from March to August for which at least 8 days were classified as thawed. For the Southern Hemisphere, we examined the periods March to August and September to February to determine the start and end of the frozen season, respectively. The range of the frozen season was defined as the period between the start and end. Second, we retrieved the snow-cover status of the cloud pixels in winter months based on their neighbouring pixels to reduce cloud obscuration[24,43]. For a cloud pixel, if all its neighbouring pixels sharing an edge were covered by snow, then we reclassified it as a pixel with snow cover. If the above criterion was not met, but both the prior and the subsequent date were classified as snow covered, then we also reclassified it as snow covered. Third, we calculated D_{sc} and D_{fwos} by combining the ground freeze/thaw status, the snow-cover status and the range of the frozen season. If a pixel had frozen ground and snow cover and its date fell within the range of the frozen season, then one day was added to D_{sc}; if a pixel had frozen ground that was not covered by snow and its date was within the range of the frozen season, then one day was added to D_{fwos}. These analyses resulted in a 5 km resolution dataset of the global patterns of D_{sc} and D_{fwos} from 1982 to 2014. Additionally, we determined another two categories: 'no frozen days', which was defined as a pixel without frozen ground throughout a year; and 'no frozen season', which was defined as a pixel without an identified start or end of the frozen season. A more detailed description can be found in Zhu et al.[24].

Assessing D_{sc} and D_{fwos} as effective indicators. To assess the accuracy of D_{sc} and D_{fwos}, we compared remote sensing-based retrievals with those calculated using in situ snow depth measurements from multiple sources (Supplementary Table 1 and Supplementary Fig. 13). We examined daily snow depth records for all stations of these datasets and selected those stations that had uninterrupted measurements for more than 20 yr from 1982 to 2014. We computed D_{sc} and D_{fwos} using procedures similar to those used for the remotely sensed retrievals (Supplementary Fig. 12) but with snow depth measurements as inputs. Coefficients obtained by regressing remotely sensed results against the corresponding station-based outputs were used to indicate their consistency. We found that remote sensing-derived D_{sc} and D_{fwos} were generally highly consistent with station-based data (Supplementary Fig. 1), but consistency differed slightly across latitude, elevation and four land-cover types (Supplementary Tables 2–4). Some of the differences between the remote sensing-derived D_{sc} and D_{fwos} and the station-based values undoubtedly are due to inaccuracy of the remote sensing. However, inaccuracy of the station-based measurements is also possible, especially given the probable heterogeneity of snow cover and frozen ground in the 5 km pixels of the remotely sensed data.

To test whether D_{sc} and D_{fwos} could serve as effective indicators of subnivium temperatures, we calculated the daily difference between ground temperatures and air temperatures (T_{diff}) using records from Snow Telemetry (SNOTEL) and Soil Climate Analysis Network (SCAN) stations (Supplementary Table 1). SNOTEL and SCAN stations are distributed across the contiguous United States and Alaska and have an encapsulated thermistor to measure soil temperature at 2, 4, 8, 20 and 40 inches of soil depth. We analysed soil temperatures at 2 inches to represent the ground surface temperatures of the subnivium, which is at the interface between snowpack and ground. We examined daily measurements and analysed data from all stations with at least 2 yr of complete records of snow depth, air temperatures

and ground temperatures, which resulted in 342 SNOTEL network stations and 113 SCAN stations. Then we compared the average T_{diff} for the period when the ground was frozen and covered with snow (the period used to determine D_{sc}) with that of the period without snow cover (the period used to determine D_{fwos}) to show their differences.

To quantify whether D_{sc} and D_{fwos} are also effective proxies of snow depth, an important determinant of the subnivium, we examined the relationships between D_{sc} and snow depth using snow depth datasets from multiple sources (Supplementary Table 1 and Supplementary Fig. 13). We calculated mean snow depth in the winter period and conducted Pearson correlation analysis between D_{sc} and mean snow depth for stations with more than 20 yr of data.

Analysing changes of global D_{sc} and D_{fwos} and their driving forces. We used the gridded high-resolution CRU datasets (1982–2015) at 0.5° resolution including monthly mean temperatures and monthly precipitation to disentangle the effects of winter climate on D_{sc} and D_{fwos} (ref. [30]). The CRU dataset is produced from existing climatologies with interpolated station anomalies at 0.5° latitude/longitude grid cells. Compared with similar gridded climate data products, the CRU dataset is more accurate, especially in regions and periods with sparser observations. The data of CRU 4.01 version were available from the Centre for Environmental Data Analysis of the United Kingdom (http://data.ceda.ac.uk//badc/cru/data/cru_ts/cru_ts_4.01/). Based on the CRU monthly data, we analysed two climate variables, winter temperatures and precipitation, both of which can potentially influence D_{sc} and D_{fwos}. Both explanatory variables were defined as the average of monthly data spanning the winter period, which was derived from the range of the frozen season.

We predicted changes in subnivium from 2015 to 2100 using the downscaled monthly CMIP5 projections from 33 GCMs under the RCP 8.5 scenario, which were available at 0.5° resolution from ftp://gdo-dcp.ucllnl.org/pub/dcp/archive/. The dataset uses the bias-correction spatial disaggregation method to downscale original GCM projections, which compares the GCM outputs with corresponding climate observations over a common period and uses information derived from the comparison to adjust future climate projections[31]. We computed time series of the climate variables, winter temperatures and precipitation, from 2015 to 2100 for future prediction.

We summarized changes in D_{sc} and D_{fwos} by land-cover type and elevation category. A yearly MODIS land-cover type product (MCD12Q1) provided the global pattern of dominant land-cover type within 0.5° grid cells. We wrote Python code that could automatically download and process all tiles of annual land-cover data covering global land area for 2001 to 2016 from the Data Pool of the Land Processes Distributed Active Archive Center (https://lpdaac.usgs.gov/tools/data-pool/). First, we reclassified annual land-cover data into four categories, including forest, grassland, cropland and barren land. We then identified the pixels with consistent land-cover type for the 16 yr. Finally, we determined the dominant land-cover type of the 0.5° grid cell, which was defined as the type whose area occupied greater than 50% of the grid area. An elevation dataset was downloaded from the Global Land One-km Base Elevation (GLOBE) database (https://www.ngdc.noaa.gov/mgg/topo/globe.html). The elevation of a 0.5° grid cell was computed by averaging the 1 km elevation data.

To estimate changes in D_{sc} and D_{fwos} through time and effects of changing temperature and precipitation on these variables, we fitted linear regression models with temporally autocorrelated errors, a method which allows for temporal correlations in the residual errors. We chose this method because the linear regression residuals were autocorrelated for many pixels, which violated the assumption of independent errors made in ordinary least squares regression and resulted in incorrect estimates of coefficients and inflated significance values. Taking a D_{sc} time series of one pixel as an example (Supplementary Fig. 14), the residuals from simple linear regression had significant autocorrelation at lag 1 (Supplementary Fig. 15), which violated the assumption of independent errors. We then fitted a time series using a linear regression model with autocorrelated errors and found that the residuals no longer showed significant autocorrelation (Supplementary Fig. 16). We further compared regression slope coefficients and their Student's t-test values for both models using D_{sc} time series from 200 random pixels. The regression slope coefficients from the model we used were generally consistent with those from linear regression, but there were slight differences (Supplementary Fig. 17). Therefore, using linear regression models with autocorrelated errors here was more conservative, because the error structures of some pixels still had significant autocorrelation.

The model we used here was written in the form

$$D(t) = b_0 + bt + c_T T(t) + c_P P(t) + \varepsilon(t) \qquad (1)$$

where $D(t)$ is either D_{sc} or D_{fwos} in year t, $T(t)$ and $P(t)$ are temperature and precipitation in year t, $\varepsilon(t)$ is the error term that incorporates temporal autocorrelation, and b_0, b, c_T and c_P are regression coefficients. The model was fitted as an AR(1) using the arima() function in the statistical language R. We calculated t-test values as $b/se\{b\}$ for a single time series in each independent pixel, and applied Student's t-test to show in maps only the pixels with significant trends or effects of climate variables at $\alpha = 0.05$.

When investigating only temporal trends in D_{sc} and D_{fwos}, $T(t)$ and $P(t)$ were excluded from the model. The equation form is

$$D(t) = b_0 + bt + \varepsilon(t) \tag{2}$$

To investigate the effects of winter temperatures and precipitation, we used the equation

$$D(t) = b_0 + c_T T(t) + c_P P(t) + \varepsilon(t) \tag{3}$$

For model fitting, we standardized $T(t)$ and $P(t)$ to have means of zero and standard deviations of one; this makes the coefficients measurements of effects sizes so that the influence of $T(t)$ and $P(t)$ on $D(t)$ can be compared. To compare the relative contributions of temperature and precipitation on changes in D_{sc} and D_{fwos}, we mapped the ratio $(|c_T| - |c_P|)/(|c_T| + |c_P|)$. This ratio varies from 1 when all of the variation is caused by temperature to -1 when all variation is caused by precipitation. When reporting the coefficients as measures of the sensitivity of $D(t)$ to actual and predicted changes in temperature and precipitation (for example, Fig. 4), the coefficients were back-transformed to the absolute scale.

To investigate the interaction between winter temperatures and precipitation, we used the equation

$$D(t) = b_0 + c_T T(t) + c_P P(t) + c_{TP} T(t)P(t) + \varepsilon(t) \tag{4}$$

where $T(t)P(t)$ is the multiplicative product of standardized temperatures and precipitation, and c_{TP} is the coefficient of the interaction between temperatures and precipitation.

We used the fitted regression models in equation (3) to predict D_{sc} and D_{fwos} in the twenty-first century for the RCP 8.5 high emissions scenario. The required model inputs, $T(t)$ and $P(t)$ for the future period, were derived by using temperature and precipitation from CMIP5 climate projections. Given the difference in spatial resolutions between our datasets and the CMIP5 climate projections, we aggregated the pixel values of D_{sc} and D_{fwos} at 5 km resolution within the grid of climatic data at the 0.5° resolution of the CMIP5 projections. For each year, we averaged the predictions of D_{sc} and D_{fwos} from the climate projections of 33 GCMs. We compared average D_{sc} and D_{fwos} during the late twenty-first century (2071–2100) with the averages during the historical period (1982–2014), and we summarized changes by latitude category, elevation category and land-cover type.

Data availability
All data used can be freely downloaded from Zenodo (https://doi.org/10.5281/zenodo.3376316) and are also available from the corresponding authors upon request.

Code availability
The Python and R code used for calculations and analyses can be accessed at GitHub (https://github.com/likai-hub/climate-change-and-subnivium-duration) and is also available from the corresponding authors upon request.

References
40. Kim, Y., Kimball, J. S., Glassy, J. & Du, J. An extended global Earth system data record on daily landscape freeze–thaw status determined from satellite passive microwave remote sensing. *Earth Syst. Sci. Data* **9**, 133–147 (2017).
41. Kim, Y., Kimball, J. S., Robinson, D. A. & Derksen, C. New satellite climate data records indicate strong coupling between recent frozen season changes and snow cover over high northern latitudes. *Environ. Res. Lett.* **10**, 084004 (2015).
42. Frei, A. et al. A review of global satellite-derived snow products. *Adv. Space Res.* **50**, 1007–1029 (2012).
43. Gao, Y., Xie, H., Yao, T. & Xue, C. Integrated assessment on multi-temporal and multi-sensor combinations for reducing cloud obscuration of MODIS snow cover products of the Pacific Northwest USA. *Remote Sens. Environ.* **114**, 1662–1675 (2010).